

# Effects of boundary-layer tripping on the acoustic tones of impinging jets

Christophe Bogey\*  and Hugo Vincent 

CNRS, Ecole Centrale de Lyon, INSA Lyon, Univ Claude Bernard Lyon 1, LMFA, UMR5509, 69130 Ecully, France

Received 20 July 2025, Accepted 19 October 2025

**Abstract** – The influence of boundary-layer tripping on the acoustic tones generated by a jet at a Mach number of 0.9 impinging on a flat plate is investigated for two nozzle-to-plate distances. Tripping the jet boundary-layer is found not to appreciably alter the frequencies but to significantly affect the levels of the tones. These effects strongly depend on the tone number and on the nozzle-to-plate distance. For a given tone, in particular, the levels can decrease or increase depending on the distance. Therefore, tripping the boundary layers of impinging jets can result to less or more noise, and cannot be considered as a reliable method to reduce noise for these jets.

**Keywords.** Jet noise, Acoustic tones, Feedback loop

## 1 Introduction

For more than fifty years since the seminal work of Crow and Champagne [1], the development of free jet flows has been known to be sensitive to the properties of the boundary layer at the nozzle exit, including its thickness, shape and turbulent state. In particular, the levels of velocity fluctuations at the nozzle exit were found to be a key parameter. Indeed, for laminar boundary layers, after the growth of Kelvin–Helmholtz (KH) instability waves, coherent structures form just downstream of the nozzle, interact with each other and merge, which is not the case for highly disturbed boundary layers. Strong pressure waves are produced by the vortex pairings, leading to very high sound pressure levels. This has been reported in several experimental and numerical studies [2–7], which cannot all be cited in this paper, where the boundary layers in the nozzle were tripped, generating disturbed exit conditions, for jets whose initial state would otherwise be laminar. Thus, boundary-layer tripping is an efficient way to reduce the noise of free jets.

The effects of the jet nozzle-exit conditions can also be expected to be significant on the noise radiated by impinging jets, which strongly differs from the noise produced by free jets. Indeed, for subsonic jets at a Mach number greater than 0.6 [8] and for supersonic, ideally expanded or shocked jets [9, 10] impinging on a plate, the acoustic field is generally dominated by tonal components due to aeroacoustic feedback loops establishing

between the nozzle exit and the plate, involving turbulent shear-layer structures convected by the flow and acoustic waves propagating in the upstream direction [11, 12]. The effects of the jet boundary-layer properties on these tones, notably in terms of emergence, frequency and amplitude, have been studied in a very limited number of studies. For instance, impinging jets at Mach numbers of 0.6 and 0.9 with untripped boundary layers of various thicknesses were simulated in Vincent and Bogey [13]. For the highest Mach number, thickening the boundary layer was found not to change the tone frequencies but to increase the amplitudes of the two dominant tones by approximately 20 dB. For the lower Mach number, it was shown to allow the generation of weak tones.

The influence of the boundary-layer tripping on the tones of impinging jets was examined in Varé and Bogey [14] for jets at Mach numbers varying between 0.6 and 1.3 impinging on a flat plate at  $8r_0$  from the nozzle exit, where  $r_0$  is the nozzle radius. Jets with untripped and tripped boundary layers, displaying laminar and highly disturbed exit conditions, respectively, were considered. For the laminar conditions, in most cases, the tones are weaker by 10–20 dB and, at Mach numbers 0.75 and 0.8, the dominant tones appear at lower frequencies, in good agreement with the experimental results of Jaunet *et al.* [15]. Therefore, tripping the jet boundary layers significantly affects the tone properties. Unfortunately, it is not possible to claim that, for another nozzle-to-plate distance, the effects would be the same as those in Varé and Bogey [14]. Furthermore, no results are

\*Corresponding author: [christophe.bogey@ec-lyon.fr](mailto:christophe.bogey@ec-lyon.fr)

**Table 1.** Nozzle-to-plate distance  $L$ , nozzle-exit peak velocity fluctuation intensities  $T_{\text{BLtrip}}$  obtained for free jets [4], and nozzle-exit peak fluctuation intensities  $u'_e/u_j$  for the impinging jets.

	L6T0%	L6T3%	L6T6%	L6T12%	L8T0%	L8T3%	L8T6%	L8T12%
$L/r_0$	6	6	6	6	8	8	8	8
$T_{\text{BLtrip}}$	0%	3%	6%	12%	0%	3%	6%	12%
$u'_e/u_j$	9.4%	8.3%	9.2%	13.7%	1.6%	5.2%	7.8%	13.4%

provided for tripped jets with weakly, not highly, disturbed nozzle-exit conditions.

Given the above, in this paper, the effects of boundary-layer tripping on the acoustic tones of impinging jets are investigated using compressible large-eddy simulations (LES), for jets at a Mach number of 0.9 impinging on a flat plate located at  $6r_0$  or  $8r_0$  of the nozzle-exit section. The jet boundary layers in the nozzle are untripped or more or less strongly tripped, in order to deal with jets which would initially be, in the absence of the plate, fully laminar or weakly, moderately or highly disturbed. The objectives will be to determine whether the effects of boundary-layer tripping on the properties of the tones change with the nozzle-to-plate distance, and whether jets with weakly tripped boundary layers generate tones resembling those from jets with untripped or strongly tripped boundary layers. The results to these questions are of importance when comparing the acoustic fields of impinging jets radiating tone components obtained from different experiments and simulations. They should also indicate whether boundary-layer tripping can or cannot be used to reduce the tonal noise of impinging jets. Finally, concerning only numerical simulations, they should allow us to assess whether the strength of the tripping device inside the nozzle is a critical parameter for such jets.

## 2 Parameters and numerical methods

### 2.1 Jet parameters

Eight isothermal round jets at a Mach number  $M = u_j/c_0 = 0.9$  and a Reynolds number  $\text{Re}_D = u_j D/\nu = 10^5$  are considered, where  $u_j$ ,  $c_0$ ,  $D = 2r_0$  and  $\nu$  are the jet velocity, the speed of sound in the ambient medium, the nozzle diameter and the kinematic molecular viscosity, as reported in Table 1. Four of them impinge on a flat plate located at a distance  $L = 6r_0$  from the nozzle-exit plane and four other ones at a distance  $L = 8r_0$ . One of them, defined as L8T0% below, was previously simulated in Varé and Bogey [14]. The jets exhaust at  $z = 0$  from a cylindrical pipe into the ambient medium at pressure  $p_0 = 10^5$  Pa and temperature  $T_0 = 293$  K. The pipe inlet is at  $z = -10r_0$ , but the flow is only computed in the nozzle for  $z \geq -2r_0$ . In the nozzle, at  $z = -2r_0$ , the radial and azimuthal velocities are set to zero, a Blasius laminar boundary layer profile of thickness  $\delta_{\text{BL}} = 0.15r_0$  is imposed for the axial velocity [16], pressure is set to  $p_0$

and temperature is obtained from a Crocco–Busemann relation.

For the two nozzle-to-plate distances, the boundary layers in the pipe are untripped in two cases, referred to as L6T0% for  $L = 6r_0$  and L8T0% for  $L = 8r_0$ . In the six other cases, referred to as L6T3%, L6T6%, L6T12% for  $L = 6r_0$  and L8T3%, L8T6% and L8T12% for  $L = 8r_0$ , the boundary layers are tripped to generate velocity fluctuations at the nozzle exit. The tripping procedure is identical to that used in Bogey *et al.* [4] to compute free jets with the same upstream conditions (Mach and Reynolds number, boundary-layer profile) and numerical methods and parameters (mesh spacings, time step) as the present jets. It consists in adding weak solenoidal fluctuations decorrelated in azimuth and time near the pipe walls at  $z = -0.95r_0$  for the cases LXT3% and LXT6% and  $z = -0.225r_0$  for LXT12%, with  $X = 6, 8$ . The amplitudes of the tripping fluctuations in LXT3%, LX6% and LXT6% are those providing peak levels of velocity fluctuations  $T_{\text{BLtrip}} = u'_e/u_j = 3\%$ ,  $6\%$  and  $12\%$  at the nozzle exit of the free jets in Bogey *et al.* [4], respectively. Therefore, the boundary layers of the present jets are untripped, or weakly, moderately or strongly tripped. It can be noted that for the free jets, the length of the potential core varies from  $9.3r_0$  in the untripped case up to  $17r_0$  in the most disturbed case. In all cases, it exceeds the two nozzle-to-plate distances of  $6r_0$  and  $8r_0$  considered in this study.

The profiles of RMS (root-mean-square) axial velocity fluctuations obtained at  $z = 0$  for the impinging jets are represented in Figure 1a for  $L = 6r_0$  and in Figure 1b for  $L = 8r_0$ . Those calculated for the corresponding free jets using the same boundary-layer tripping [4] are also shown. In all cases, for a given tripping magnitude  $T_{\text{BLtrip}}$ , the levels are higher in the impinging jets than in the free jet. As discussed in Vincent and Bogey [13], this is due to the presence of intense upstream-propagating guided jet waves (GJW) [17–20] closing the feedback loops in impinging jets [8, 21, 22], radiating in far field in the upstream direction [23]. These waves result in strong fluctuations in the jet outside the boundary layer, e.g. at  $r = 0.8r_0$ , but also inside, implying that, even when they are untripped or weakly tripped, the boundary layers are substantially excited at the nozzle exit. The peak fluctuation intensities for the impinging jets thus vary between 8.3% and 13.7% for  $L = 6r_0$  and between 1.6% and 13.4% for  $L = 8r_0$ . They are much stronger in the first case than in the second, suggesting that the jets are more resonant and produce more noise for the shorter nozzle-to-plate distance.

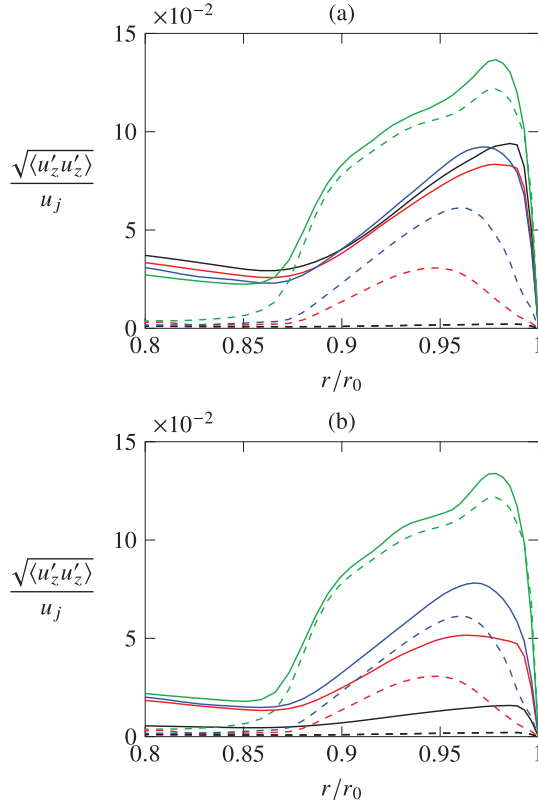


**Figure 1.** Nozzle-exit profiles of the RMS values of axial velocity fluctuations for (a) — L6T0%, — L6T3%, — L6T6%, — L6T12% and (b) — L8T0%, — L8T3%, — L8T6%, — L8T12%; (dashed lines) profiles for the corresponding free jets [4] with  $T_{BLtrip} = 0\%, 3\%, 6\%$  and  $12\%$ .

## 2.2 Numerical methods and parameters

The LES are carried out by solving the unsteady compressible Navier–Stokes equations in cylindrical coordinates  $(r, \theta, z)$  using the same numerical framework as in recent simulations of free [18, 19] and impinging [13, 14, 24, 25] round jets. Fourth-order eleven-point centered finite differences are used for spatial discretization and a second-order six-stage Runge–Kutta algorithm is implemented for time integration. A six-order centered filter is applied explicitly to the flow variables every time step to remove grid-to-grid oscillations. The filtering is also employed as a subgrid-scale high-order dissipation model to relax turbulent energy from scales at wave numbers close to the grid cut-off wave number while leaving larger scales mostly unaffected [26]. The axis singularity is taken into account by the method of Mohseni and Colonius [27], and the derivatives in the azimuthal direction around the axis are calculated at coarser resolutions than permitted by the grid [28]. Near the plate, for  $z \geq 3r_0$  for L8T0% [14] and for  $z > L - 3r_0$  for the other jets, a second-order shock-capturing filtering is used to avoid the development of Gibbs oscillations near the shocks that may appear near the plate [29]. Non-centered finite differences and filters are used near

the pipe walls and the grid boundaries. At the upstream and lateral boundaries, radiation conditions of Tam and Dong [30] are applied and sponge zones combining mesh stretching and Laplacian filtering are implemented. No-slip adiabatic wall boundary conditions are imposed to the plate and to the pipe walls.

The characteristics of the LES mesh grids in the  $(z, r)$  section depend on the nozzle-to-plate distance. They are detailed in Vincent and Bogey [13] for  $L = 6r_0$  and in Varé and Bogey [14] for  $L = 8r_0$ . Excluding the sponge zones implemented between  $z = -20r_0$  and  $z = -10r_0$  and between  $r = 15r_0$  and  $r = 30r_0$ , they extend axially from  $z = -10r_0$  down to  $z = L$  and radially out to  $r = 15r_0$ . The minimum axial and radial mesh spacings are equal to  $\Delta z = 0.0072r_0$  near the nozzle exit and near the plate and to  $\Delta r = 0.0036r_0$  at  $r = r_0$ . The grids contain  $N_z = 1122$  points for  $L = 6r_0$  and 1296 points for  $L = 8r_0$  in the axial direction and  $N_r = 559$  points in the radial direction. In the azimuth, there are  $N_\theta = 256$  points for the jets with untripped boundary layers and  $N_\theta = 1024$  points for the other ones. Thus, there are between 160 and 740 million points in the grids.

In all simulations, the time step is set to  $\Delta t = 0.7\Delta r(r = r_0)/c_0$  to ensure numerical stability. After transient periods of  $500r_0/u_j$  for the jets with untripped boundary layers and of  $300r_0/u_j$  for the other jets, density, velocity components and pressure are recorded in the azimuthal planes  $\theta = 0, \pi/4, \pi/2$  and  $3\pi/4$  during a time of  $1500r_0/u_j$  for  $L = 6r_0$  and a time of  $625r_0/u_j$  for  $L = 8r_0$ . The sampling frequency allows to compute spectra up to a Strouhal number  $St_D = fD/u_j = 12.8$ , where  $f$  is the frequency. The Fourier coefficients estimated over the section  $(z, r)$  for the azimuthal modes  $n_\theta = 0$  to 3, where  $n_\theta$  is the azimuthal wavenumber, are also saved at a halved sampling frequency.

## 3 Results

Snapshots of vorticity norm and pressure fluctuations are first provided in Figure 2 for the eight jets. In the mixing layers, near the nozzle, vortical structures appear in the untripped cases in Figures 2a and 2e, but are less difficult to observe as the jet boundary layers are tripped, as expected. In the vicinity of the flat plate, the shear layers have not merged indicating that in all cases the nozzle-to-plate distance is too short to allow the jet potential core to close. They contain large-scale turbulent structures, symmetric with respect to the jet axis, which may indicate that the flow development is dominated by an axisymmetric oscillation mode.

To characterize the flow topology, the variations of  $\langle \rho \rangle / \rho_0 - 1$  on the jet axis, where  $\langle \rho \rangle$  and  $\rho_0$  are the mean and ambient densities, are plotted in Figure 3a for  $L = 6r_0$  and in Figure 3b for  $L = 8r_0$ . For  $L = 6r_0$ , shocks are observed in the jets, in particular close to the plate, and they are of similar strength in the four cases. In contrast, for  $L = 8r_0$ , the shocks are weaker as  $T_{BLtrip}$  decreases, and even disappear for L8T0%. Given that the



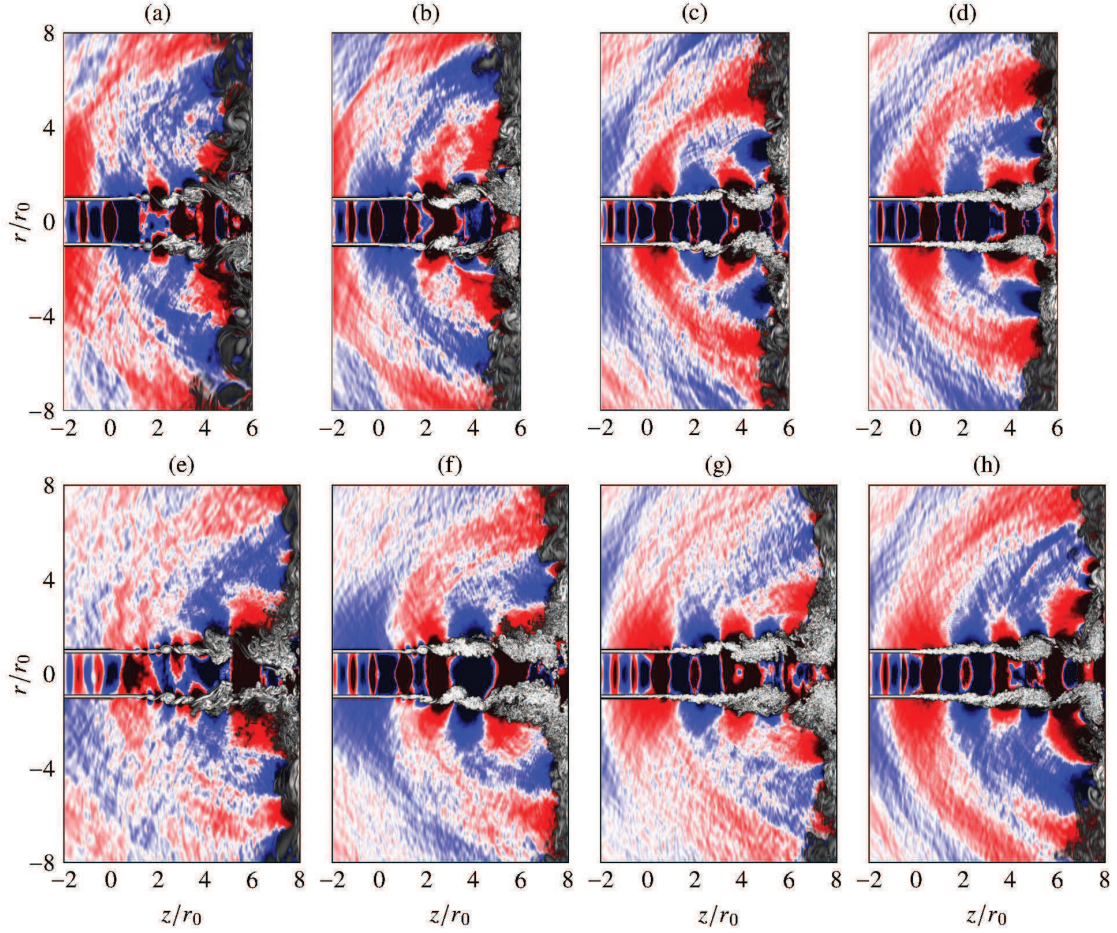


**Figure 2.** Vorticity norm and pressure fluctuations in the  $(z, r)$  plane for (a) L6T0%, (b) L6T3%, (c) L6T6%, (d) L6T12%, (e) L8T0%, (f) L8T3%, (g) L8T6% and (h) L8T12%. The color scales range from 0 to  $12u_j/r_0$  for vorticity, from black to white, and between  $\pm 0.04p_0$  for pressure, from blue to red. The nozzle lips are in black.

presence of a standoff shock near the plate can affect the aeroacoustic feedback loops in impinging jets [31, 32] and that the upstream-travelling acoustic waves closing the loops can be generated by a shock-leakage phenomenon through the jet shear layer [24, 33] as in screeching jets, the tone generation mechanisms are likely to be of the same nature in the four jets for  $L = 6r_0$ , but to differ in the jets for  $L = 8r_0$ .

In the pressure fields of Figure 2, the levels are very high inside the jet potential core, where GJW are trapped. Outside the jet, low-frequency circular waves originating from the jet impingement region on the plate are observed. In particular, regularly-spaced wavefronts, which may be related to an axisymmetric tonal noise component, are visible. For  $T_{BLtrip} = 12\%$ , in Figures 2d and 2h, the amplitudes of the circular waves are similar for  $L = 6r_0$  and  $L = 8r_0$ . As the value of  $T_{BLtrip}$  decreases, they do not seem to change much for  $L = 6r_0$  in Figures 2a–2d, but they are significantly lower for  $L = 8r_0$  in Figures 2e–2h. Therefore, the influence of the boundary-layer tripping on the amplitudes of the acoustic tones depends on the nozzle-to-plate distance.

The properties of the sound field in the upstream direction are characterized in the jet acoustic near field close to the nozzle exit. This is very often the case in jet noise experiments, for instance on screech tones [34] and on guided jet waves [7, 35], due to the difficulty of implementing microphones in the jet acoustic far field upstream of the nozzle because of the presence of the settling chamber and of reflective surfaces. The position considered in this work is located in the nozzle-exit section outside the jet, at  $z = 0$  and  $r = 1.5r_0$  as in previous numerical studies on impinging jet noise [13, 14, 24, 25].

The sound pressure levels (SPL) obtained at this position are represented as a function of Strouhal number in Figure 4a for  $L = 6r_0$  and in Figure 4b for  $L = 8r_0$ . The SPL for the corresponding isothermal free jet [18] with  $T_{BLtrip} = 9\%$  are also plotted to show the footprints left by the upstream-propagating GJW in the near-nozzle spectra in absence of a flat plate. These footprints consist of peaks with a saw-tooth shape, emerging within the allowable frequency ranges of the upstream-propagating free-stream GJW [7, 18, 36–38]. In particular, the first and second peaks at  $St_D \simeq 0.4$  and  $0.7$  are due to GJW of the first radial modes for  $n_\theta = 0$  and  $n_\theta = 1$ , respectively.

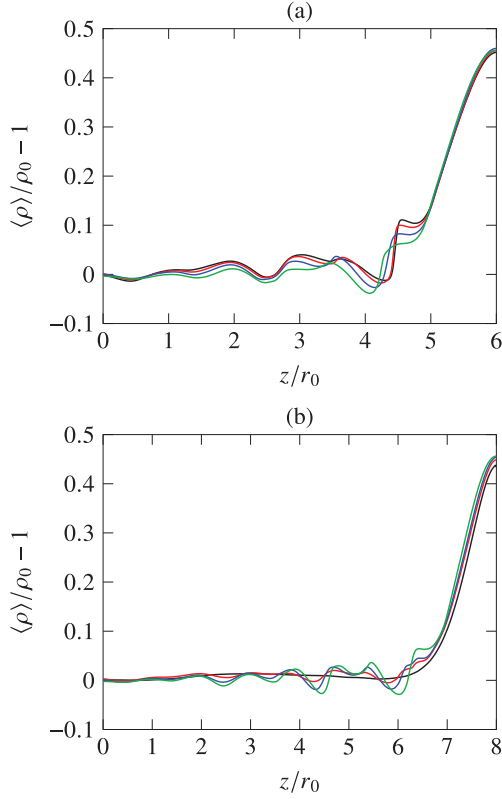


**Figure 3.** Centerline profiles of mean density  $\langle \rho \rangle / \rho_0 - 1$  for (a) — L6T0%, — L6T3%, — L6T6%, — L6T12% and (b) — L8T0%, — L8T3%, — L8T6%, — L8T12%.

Concerning the impinging jets, their spectra exhibit very intense tones, emerging 30–40 dB above the broadband noise levels, resulting from feedback loops between the nozzle lip and the plate. Their frequencies do not seem to change appreciably with the magnitude of the boundary-layer tripping. In all cases, a dominant tone is observed around  $St_D = 0.4$ , generating higher harmonics, and strong tones are also found near  $St_D = 0.7$ . Regarding the amplitudes of the tones, they appear to significantly vary with  $T_{BLtrip}$ , differently according to the nozzle-to-plate distance, as will be described later.

To illustrate the azimuthal structure of the jet acoustic fields, the spectra obtained using a Fourier decompositions of the pressure signals at  $z = 0$  and  $r = 1.5r_0$  in the azimuthal direction are reported in Figure 5a for L6T6% and in Figure 5b for L8T6%. It appears clearly that the dominant tone around  $St_D = 0.4$  and the weaker ones at lower  $St_D$  result from axisymmetric acoustic waves, and that the tones around  $St_D = 0.7$  are due to waves belonging to the mode  $n_\theta = 1$ . This is expected considering the allowable frequency ranges of the upstream-propagating free-stream GJW modes for  $n_\theta = 0$  and 1 for jets at a Mach number of 0.9 [7, 18].

The Strouhal numbers of the first and second (non-harmonic) tones obtained for modes  $n_\theta = 0$  and  $n_\theta = 1$  in the spectra are presented as a function of  $T_{BLtrip}$  in Figure 6a for  $L = 6r_0$  and in Figure 6b for  $L = 8r_0$ .

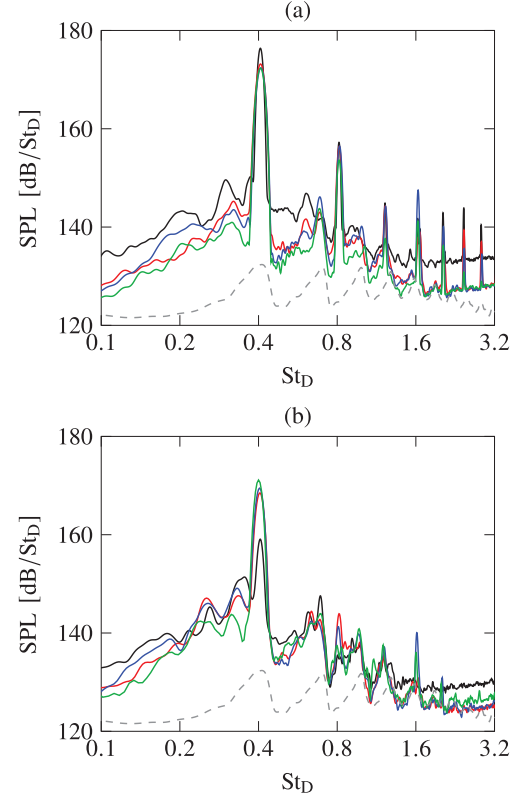


**Figure 4.** Sound pressure levels at  $z = 0$  and  $r = 1.5r_0$  for (a) — L6T0%, — L6T3%, — L6T6%, — L6T12% and (b) — L8T0%, — L8T3%, — L8T6%, — L8T12%; --- SPL + 10 dB at  $z = 0$  and  $r = 1.5r_0$  for the corresponding free jet [18] with  $T_{BLtrip} = 9\%$ .

The frequencies predicted for an aeroacoustic feedback loop [11, 12], given by

$$\frac{L}{u_c} + \frac{L}{u_{\text{sound}}} = \frac{N}{f} \quad (1)$$

assuming an average convection velocity  $u_c = (2/3)u_j$  for the shear-layer structures between the nozzle and the plate and a phase velocity of  $u_{\text{sound}} = c_0$  for the acoustic waves closing the loop are also displayed for feedback mode numbers  $N \geq 1$ . The first assumption is the classical approximation used in jet modelling, which provided fairly good predictions of the impinging tone frequencies in previous numerical studies [14, 24, 25]. The second assumption is justified by the fact that the upstream-travelling GJW closing the feedback loops are nearly sonic, regardless of the jet Mach number [39]. Values of  $u_c$  and  $u_{\text{sound}}$  could be calculated for each tone from the LES unsteady fields using velocity cross-correlations and wavenumber-frequency analysis of the pressure fields. However, the values obtained would not be necessarily very accurate given that the convection velocity of the turbulent structures varies appreciably between the nozzle and the plate and is not easy to calculate near the plate [21] and that the short nozzle-to-plate distances in this study result in a poor wavenumber resolution in the wavenumber-frequency spectra [13]. It has

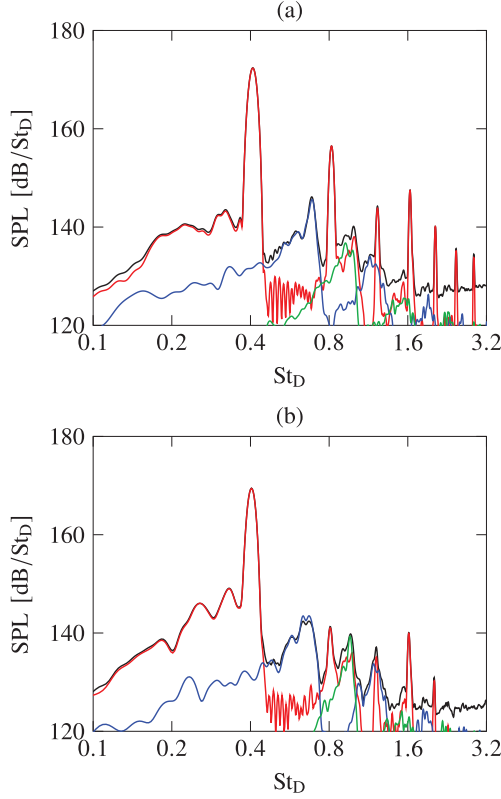


**Figure 5.** Sound pressure levels at  $z = 0$  and  $r = 1.5r_0$  for (a) L6T6% and (b) L8T6%: — full, —  $n_\theta = 0$ , —  $n_\theta = 1$ , —  $n_\theta = 2$ .

finally been checked that using slightly different values for  $u_c$  or  $u_{\text{sound}}$  in equation (1) does not significantly change the predicted frequencies.

For both nozzle-to-plate distances, the Strouhal numbers of the four tones do not vary much with the amplitude of the boundary-layer tripping. Consequently, the tones remain associated with the same four feedback mode numbers. More precisely, as reported in the figure caption, the tones for  $L = 6r_0$  in Figure 6a can be related to modes  $N = 2$  and  $3$  for  $n_\theta = 0$  and  $N = 4$  and  $5$  for  $n_\theta = 1$ , and those for  $L = 8r_0$  in Figure 6b to modes  $N = 3$  and  $4$  for  $n_\theta = 0$  and  $N = 6$  and  $7$  for  $n_\theta = 1$ . The differences between the tone frequencies obtained in the LES and those predicted by equation (1) can be attributed to the approximations  $u_c = (2/3)u_j$  and  $u_{\text{sound}} = c_0$  discussed above.

To characterize the effects of the boundary-layer tripping on the tone prominence, the levels of the two first tones for  $n_\theta = 0$  and  $n_\theta = 1$  are presented as a function of  $T_{\text{BLtrip}}$  in Figure 7a for  $L = 6r_0$  and in Figure 7b for  $L = 8r_0$  using the same symbols as in Figures 6a and 6b. The tone levels significantly differ between the untripped and the tripped cases  $T_{\text{BLtrip}} = 0\%$  and  $T_{\text{BLtrip}} = 3\%$ , but vary in a rather limited manner with  $T_{\text{BLtrip}}$  in the tripped cases. Except for that, the results strongly depend on the nozzle-to-plate distance and on the tone number. For the axisymmetric mode, for  $L = 6r_0$ , the levels of the

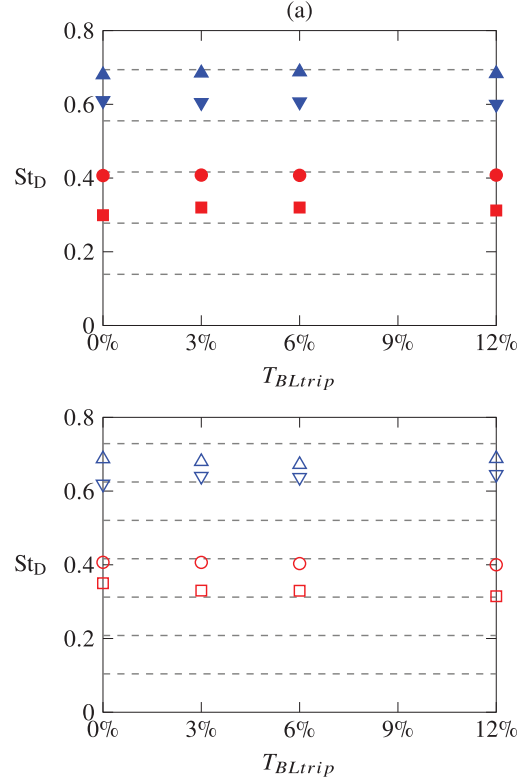


**Figure 6.** Strouhal numbers as a function of  $T_{\text{BLtrip}}$  of the tones: (a) for  $L = 6r_0$  with  $\blacksquare$  ( $n_\theta = 0$ ,  $N = 2$ ),  $\bullet$  ( $n_\theta = 0$ ,  $N = 3$ ),  $\blacktriangledown$  ( $n_\theta = 1$ ,  $N = 4$ ) and  $\blacktriangle$  ( $n_\theta = 1$ ,  $N = 5$ ), (b) for  $L = 8r_0$  with  $\square$  ( $n_\theta = 0$ ,  $N = 3$ ),  $\circ$  ( $n_\theta = 0$ ,  $N = 4$ ),  $\nabla$  ( $n_\theta = 1$ ,  $N = 6$ ),  $\triangledown$  ( $n_\theta = 1$ ,  $N = 7$ ) and  $\triangle$  ( $n_\theta = 1$ ,  $N = 8$ ); --- Strouhal numbers obtained using the feedback model for  $N \geq 1$ .

first and the second tones decrease by 4.8 dB and 8.8 dB between  $T_{\text{BLtrip}} = 0\%$  and  $T_{\text{BLtrip}} = 12\%$ , whereas for  $L = 8r_0$ , they increase by 13.4 dB for the first tone and decrease by 7.1 dB for the second. The low level of the first tone for L8T0% may be explained by the absence of shocks in the jet near the plate in this case, preventing the generation of upstream-travelling acoustic waves by a shock-leakage mechanism. For both  $L = 6r_0$  and  $L = 8r_0$ , the feedback mode number attributed to the dominant tone, obtained for the axisymmetric mode, does not change with  $T_{\text{BLtrip}}$ . For the helical mode  $n_\theta = 1$ , for  $L = 6r_0$ , the levels of the tones related to the mode numbers  $N = 4$  and  $N = 5$  decrease by 12.2 dB and increase by 5.7 dB, respectively. Thus, the tone for  $N = 4$  is predominant for  $T_{\text{BLtrip}} = 0\%$ , and that for  $N = 5$  prevails for  $T_{\text{BLtrip}} \geq 3\%$ . Finally, for  $n_\theta = 1$  and  $L = 8r_0$ , the levels of the two first tones are similar and neither greatly vary nor monotonously evolve with  $T_{\text{BLtrip}}$ .

## 4 Conclusions

In this paper, the influence of boundary-layer tripping on the acoustic tones generated by a jet at a Mach number of 0.9 impinging on a flat plate is investigated for two

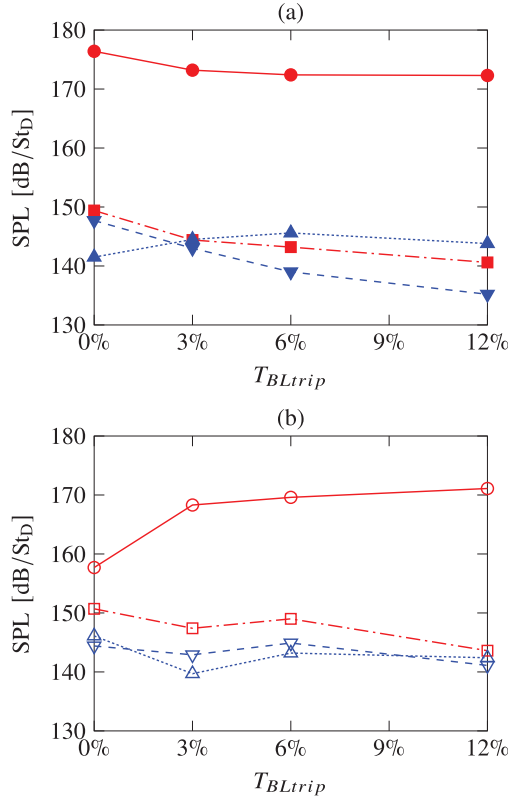


**Figure 7.** Sound pressure levels as a function of  $T_{BLtrip}$  of the tones: (a) for  $L = 6r_0$  with  $\blacksquare$  ( $n_\theta = 0$ ,  $N = 2$ ),  $\bullet$  ( $n_\theta = 0$ ,  $N = 3$ ),  $\blacktriangledown$  ( $n_\theta = 1$ ,  $N = 4$ ) and  $\blacktriangle$  ( $n_\theta = 1$ ,  $N = 5$ ), (b) for  $L = 8r_0$  with  $\square$  ( $n_\theta = 0$ ,  $N = 3$ ),  $\circ$  ( $n_\theta = 0$ ,  $N = 4$ ),  $\triangledown$  ( $n_\theta = 1$ ,  $N = 6$ ) and  $\triangle$  ( $n_\theta = 1$ ,  $N = 7$ ).

nozzle-to-plate distances. Tripping the jet boundary-layer is found not to appreciably alter the frequencies of the tones. This can be attributed to the fact that, regardless of the nozzle-exit boundary-layer state, the tones can only emerge at the frequencies allowing the establishment of an aeroacoustic feedback loop, lying within the frequency ranges of the upstream-propagating free-stream GJW. In contrast, boundary-layer tripping can significantly affect the levels of the tones. These effects strongly depend on the tone number and on the nozzle-to plate distance. For the dominant tone, for instance, the levels are observed to dramatically decrease for the shortest distance but to increase for the largest one. The discrepancy is most likely due to the fact that changing the nozzle-to-plate distance modifies the various ingredients of the aeroacoustic feedback loop responsible for the selection and the emergence of tones. They include, among others, the power gains of the KH instability waves between the nozzle and the plate, the positions of the frequencies possible for an aeroacoustic feedback loop within the frequency ranges of the upstream-propagating free-stream GJW, in which the amplitudes of the latter on the nozzle-lip line vary, and the presence and the position of a standoff shock just upstream of the plate. Therefore, contrary to free jets for which boundary-layer tripping necessarily leads to less noise, tripping the boundary layers of impinging

jets can result to less or more noise, and hence cannot be considered as a reliable method to reduce noise. Finally, it should be noted that similar results are obtained for the present impinging jets when the boundary layers are weakly or highly tripped. This suggests that the magnitude of the tripping is not a key parameter for these jets, where resonance phenomena occur.

### Acknowledgments

This work was granted access to the HPC resources of PMCS2I (Pôle de Modélisation et de Calcul en Sciences de l'Ingénieur de l'Information) of Ecole Centrale de Lyon and to the resources of IDRIS (Institut du Développement et des Ressources en Informatique Scientifique) under the allocation 2023-2a0204 made by GENCI (Grand Equipement National de Calcul Intensif). It was performed within the framework of the LABEX CeLyA (ANR-10-LABX-0060) of Université de Lyon, within the program *Investissements d'Avenir* (ANR-16-IDEX-0005) operated by the French National Research Agency (ANR). For the purpose of Open Access, a CC-BY public copyright licence has been applied by the authors to the present document and will be applied to all subsequent versions up to the Author Accepted Manuscript arising from this submission.

### Funding

The second author was supported by the FUI25 CALM-AA (CiblAge des sources par voie Logicielle et Méthodes inverses pour l'AéroAcoustique) regional project, co-financed by the European regional development fund.

### Conflicts of interest

The authors report no conflict of interest.

### Data availability statement

Data are available on request from the authors.

### References

1. S.C. Crow, F.H. Champagne: Orderly structure in jet turbulence. *Journal of Fluid Mechanics* 48 (1971) 547–591.
2. K.B.M.Q. Zaman: Effect of initial condition on subsonic jet noise. *AIAA Journal* 23, 9 (1985) 1370–1373.
3. J.E. Bridges, A.K.M.F. Hussain: Roles of initial conditions and vortex pairing in jet noise. *Journal of Sound and Vibration* 117, 2 (1987) 289–311.
4. C. Bogey, O. Marsden, C. Bailly: Influence of initial turbulence level on the flow and sound fields of a subsonic jet at a diameter-based Reynolds number of  $10^5$ . *Journal of Fluid Mechanics* 701 (2012) 352–385.
5. K.B.M.Q. Zaman: Effect of initial boundary-layer state on subsonic jet noise. *AIAA Journal* 50, 8 (2012) 1784–1795.
6. R.A. Fontaine, G.S. Elliott, J.M. Austin, J.B. Freund: Very near-nozzle shear-layer turbulence and jet noise. *Journal of Fluid Mechanics* 770 (2015) 27–51.
7. G.A. Brès, P. Jordan, V. Jaunet, M. Le Rallic, A.V.G. Cavalieri, A. Towne, S.K. Lele, T. Colonius, O.T. Schmidt: Importance of the nozzle-exit boundary-layer state in subsonic turbulent jets. *Journal of Fluid Mechanics* 851 (2018) 83–124.
8. C.K.W. Tam, K.K. Ahuja: Theoretical model of discrete tone generation by impinging jets. *Journal of Fluid Mechanics* 214 (1990) 67–87.



9. B. Henderson, A. Powell: Experiments concerning tones produced by an axisymmetric choked jet impinging on flat plates. *Journal of Sound and Vibration* 168, 2 (1993) 307–326.
10. A. Krothapalli, E. Rajkuperan, F. Alvi, L. Lourenco: Flow field and noise characteristics of a supersonic impinging jet. *Journal of Fluid Mechanics* 392 (1999) 155–181.
11. C.M. Ho, N.S. Nosseir: Dynamics of an impinging jet. Part 1. The feedback phenomenon. *Journal of Fluid Mechanics* 105 (1981) 119–142.
12. A. Powell: The sound-producing oscillations of round under-expanded jets impinging on normal plates. *The Journal of the Acoustical Society of America* 83, 2 (1988) 515–533.
13. H. Vincent, C. Bogey: Influence of the boundary-layer thickness on the generation of tonal noise components by subsonic impinging jets. *Journal of Fluid Mechanics* 985 (2024) A26.
14. M. Varé, C. Bogey: Acoustic tones generated by impinging jets: differences between laminar and highly-disturbed nozzle-exit boundary layers. *International Journal of Aeroacoustics* 23, 3, 4 (2024) 342–362.
15. V. Jaunet, M. Mancinelli, P. Jordan, A. Towne, D.M. Edgington-Mitchell, G. Lehnasch, S. Girard: Dynamics of round jet impingement. *AIAA Paper* 2019-2769, 2019.
16. C. Bogey, R. Sabatini: Effects of nozzle-exit boundary-layer profile on the initial shear-layer instability, flow field and noise of subsonic jets. *Journal of Fluid Mechanics* 876 (2019) 288–325.
17. C.K.W. Tam, F.Q. Hu: On the three families of instability waves of high-speed jets. *Journal of Fluid Mechanics* 201 (1989) 447–483.
18. C. Bogey: Acoustic tones in the near-nozzle region of jets: characteristics and variations between Mach numbers 0.5 and 2. *Journal of Fluid Mechanics* 921 (2021) A3.
19. C. Bogey: Interactions between upstream-propagating guided jet waves and shear-layer instability waves near the nozzle of subsonic and nearly ideally expanded supersonic free jets with laminar boundary layers. *Journal of Fluid Mechanics* 949 (2022) A41.
20. P.A.S. Nogueira, A.V.G. Cavalieri, E. Martini, A. Towne, P. Jordan, D. Edgington-Mitchell: Guided-jet waves. *Journal of Fluid Mechanics* 999 (2024) A47.
21. C. Bogey, R. Gojon: Feedback loop and upwind-propagating waves in ideally-expanded supersonic impinging round jets. *Journal of Fluid Mechanics* 823 (2017) 562–591.
22. D. Edgington-Mitchell: Aeroacoustic resonance and self-excitation in screeching and impinging supersonic jets – a review. *International Journal of Aeroacoustics* 18, 2, 3 (2019) 118–188.
23. C. Bogey: Tones in the acoustic far field of jets in the upstream direction. *AIAA Journal* 60, 4 (2022) 2397–2406.
24. M. Varé, C. Bogey: Presence and properties of acoustic peaks near the nozzle of a rocket jet impinging on a plate. *Acta Acustica* 6 (2022) 36.
25. M. Varé, C. Bogey: Mach number dependence of tone generation by impinging round jets. *AIAA Journal* 61, 8 (2023) 3551–3565.
26. D. Fauconnier, C. Bogey, E. Dick: On the performance of relaxation filtering for large-eddy simulation. *Journal of Turbulence* 14, 1 (2013) 22–49.
27. K. Mohseni, T. Colonius: Numerical treatment of polar coordinate singularities. *Journal of Computational Physics* 157, 2 (2000) 787–795.
28. C. Bogey, N. de Cacqueray, C. Bailly: Finite differences for coarse azimuthal discretization and for reduction of effective resolution near origin of cylindrical flow equations. *Journal of Computational Physics* 230, 4 (2011) 1134–1146.
29. C. Bogey, N. de Cacqueray, C. Bailly: A shock-capturing methodology based on adaptive spatial filtering for high-order non-linear computations. *Journal of Computational Physics* 228, 5 (2009) 1447–1465.
30. C.K.W. Tam, Z. Dong: Radiation and outflow boundary conditions for direct computation of acoustic and flow disturbances in a nonuniform mean flow. *Journal of Computational Acoustics* 4, 2 (1996) 175–201.
31. C.Y. Kuo, A.P. Dowling: Oscillations of a moderately underexpanded choked jet impinging upon a flat plate. *Journal of Fluid Mechanics* 315 (1996) 267–291.
32. B. Henderson, J. Bridges, M. Wernet: An experimental study of the oscillatory flow structure of tone-producing supersonic impinging jets. *Journal of Fluid Mechanics* 542 (2005) 115–137.
33. D.M. Edgington-Mitchell, J.L. Weightman, S. Mazharmanesh, P. Nogueira: Vortices, shocks and non-linear acoustic waves: the ingredients for resonance in impinging compressible jets. *Journal of Fluid Mechanics* 1015 (2025) A56.
34. J. Panda, G. Raman, K.B.M.Q. Zaman: Underexpanded screeching jets from circular, rectangular, and elliptic nozzles. Technical Report 20040074328, NASA TM, 2004.
35. K. Zaman, J. Bridges, P. Upadhyay, C. Brown: “Trapped wave” resonance tones radiated in the forward arc of high-speed jets. Technical Report 20240009873, NASA TM, 2024.
36. T. Suzuki, T. Colonius: Instability waves in a subsonic round jet detected using a near-field phased microphone array. *Journal of Fluid Mechanics* 565 (2006) 197–226.
37. K.B.M.Q. Zaman, A.F. Fagan, P. Upadhyay: Pressure fluctuations due to “trapped waves” in the initial region of compressible jets. *Journal of Fluid Mechanics* 931 (2022) A30.
38. C. Bogey: Guided-jet waves generated by an acoustic source in a jet at a mach number of 0.95. *Journal of Fluid Mechanics* (2025). To appear; see also *AIAA Paper* 2025-3078.
39. C.K.W. Tam, T.D. Norum: Impingement tones of large aspect ratio supersonic rectangular jets. *AIAA Journal* 30, 2 (1992) 304–311.